

Liquid-gas instability and superfluidity in nuclear matter

Masayuki Matsuzaki*

Department of Physics, Graduate School of Sciences,

Kyushu University, Fukuoka 812-8581, Japan and

Department of Physics, Fukuoka University of Education,

Munakata, Fukuoka 811-4192, Japan[†]

(Dated: February 7, 2008)

Abstract

We study effects of the medium polarization on superfluidity in symmetric nuclear matter in a relativistic formalism. An effect of the liquid-gas instability is emphasized. We examine two types of decomposition of the nucleon propagator; the standard Feynman-density and the particle-hole-antiparticle ones. In both cases, the medium polarization effect is determined by a characteristic cancellation among the σ , the longitudinal ω , and the σ - ω mixed polarizations. The instability leads to increase of pairing gap. Around the saturation density that is free from the instability the medium polarization enhances pairing gap in the former case whereas reduces in the latter. At the lowest density that is also free from the instability the gap increases in both cases.

PACS numbers: 21.65.+f, 21.60.-n, 21.60.Jz

*matsuza@fukuoka-edu.ac.jp

[†]permanent address

I. INTRODUCTION

Superfluidity in nuclear matter has long been studied mainly in pure neutron matter from a view point of neutron-star physics such as cooling rates and glitch phenomena [1]. In addition, that in nuclear matter with finite Z/N ratio is also becoming of interest as basic information for the structure theory of finite nuclei, since recent development of RI-beam experiments makes it possible to study $N \simeq Z$ medium-heavy nuclei and neutron-rich light nuclei.

At present, there are two ways to describe the fundamental properties such as the saturation property of the finite-density nuclear many-body system; the non-relativistic and the relativistic models. They are understood as describing observed properties almost equally. Among them, we here adopt the latter. The origin of quantum hadrodynamics (QHD) can be traced back to Duerr's relativistic nuclear model [2] that reformulated a non-relativistic field theoretical model of Johnson and Teller [3]. Since Chin and Walecka succeeded in reproducing the saturation property of symmetric nuclear matter within the mean-field approximation [4, 5, 6], QHD has not only been evolving beyond the mean-field approximation as a many-body theory but also been enlarging its objects as a nuclear structure model such as infinite matter \rightarrow spherical \rightarrow deformed \rightarrow rotating nuclei [7, 8]. These successes indicate that the particle-hole channel interaction in QHD is realistic. In contrast, relativistic nuclear structure calculations with pairing done so far have been using particle-particle channel interactions borrowed from non-relativistic models and therefore the particle-particle channel in QHD has not been studied fully even in infinite matter. Aside from practical successes, this situation is unsatisfactory theoretically. Therefore, in this paper, we present an effort to derive an in-medium particle-particle interaction that is consistent with the relativistic mean field (RMF) although only infinite matter can be discussed at the present stage.

Up to now, there have been a lot of non-relativistic studies of pairing in nuclear matter. As for the particle-particle interaction entering into the gap equation, many authors adopted bare interactions whereas others adopted renormalized ones such as G -matrices. Although, in the medium, renormalized interactions would be used intuitively, following reasons support the use of bare interactions: (1) The Green's function formalism leads to the sum of the irreducible diagrams [9, 10], and its lowest order is the bare interaction. (2) The gap equation itself implies the short-range correlation [1, 10, 11, 12]. In general, medium renormalizations

are expected to enhance the gap by reducing the short-range repulsion. An interesting exception is the Gogny force. This is known to reproduce the pairing properties given by bare interactions at least at low densities [13]. Anyway, as a next step, polarization diagrams should be considered. In the non-relativistic framework, a lot of works have been done to study medium polarization effects on superfluidity in neutron matter [14, 15, 16, 17, 18, 19, 20, 21, 22]. All of them concluded that the medium polarization reduces pairing gap significantly. A recent ab initio calculation [23], however, claimed that the polarization effect is weak. Studies of polarization effects on symmetric nuclear matter have just begun recently. Reference [24] reported that the gap *increases* substantially. At the low density limit, Ref. [19] discussed that in the Fermi systems with 4 species the medium polarization enhances the gap.

Symmetric matter was also studied in the relativistic framework [25, 26]. Both of these references reported that the vacuum polarization reduces the gap while the latter reported that the medium polarization enhances the gap. References [26, 27] discussed that the increase of the gap is related to the existence of an instability. This is known as the liquid-gas instability [28, 29, 30].

Thus, in this paper, we investigate the liquid-gas instability and its effects on superfluidity in symmetric nuclear matter. Results on pure neutron matter are also mentioned briefly. Preliminary results were reported in Ref. [31].

II. LIQUID-GAS INSTABILITY IN RELATIVISTIC RANDOM PHASE APPROXIMATION

We begin with the ordinary σ - ω model Lagrangian density,

$$\begin{aligned}
\mathcal{L} = & \bar{\psi}(i\gamma_\mu\partial^\mu - M)\psi \\
& + \frac{1}{2}(\partial_\mu\sigma)(\partial^\mu\sigma) - \frac{1}{2}m_\sigma^2\sigma^2 - \frac{1}{4}\Omega_{\mu\nu}\Omega^{\mu\nu} + \frac{1}{2}m_\omega^2\omega_\mu\omega^\mu \\
& + g_\sigma\bar{\psi}\sigma\psi - g_\omega\bar{\psi}\gamma_\mu\omega^\mu\psi, \\
& \Omega_{\mu\nu} = \partial_\mu\omega_\nu - \partial_\nu\omega_\mu.
\end{aligned} \tag{1}$$

Here ψ , σ , and ω are the nucleon, the σ meson, and the ω meson fields, respectively, M , m_σ , and m_ω are their masses, and g_σ and g_ω are the nucleon-meson coupling constants.

The relativistic mean field approximation is carried out by replacing the meson fields in the coupled equations of motion by their expectation values as

$$\begin{aligned}\sigma &\rightarrow \langle \sigma \rangle = \sigma_0, \\ \omega_\mu &\rightarrow \langle \omega_\mu \rangle = \delta_{\mu 0} \omega_0.\end{aligned}\tag{2}$$

Then the nucleon effective mass (Dirac mass) equation is given by

$$\begin{aligned}M^* &= M - g_\sigma \sigma_0 \\ &= M - \frac{g_\sigma^2}{m_\sigma^2} \frac{\lambda}{\pi^2} \int_0^{k_F} \frac{M^*}{\sqrt{k^2 + M^{*2}}} k^2 dk,\end{aligned}\tag{3}$$

where the isospin factor $\lambda = 2$ and 1 indicate symmetric nuclear matter and pure neutron matter, respectively. The Fermi momentum is related to the baryon density as

$$\rho_B = \frac{\lambda}{3\pi^2} k_F^3.\tag{4}$$

Properties of normal fluid, zero temperature matter of a given density is completely determined by the above effective mass equation (3). The so-called saturation curve or the equation of state is given by the binding energy per nucleon, $E/A - M = \mathcal{E}/\rho_B - M$, as a function of ρ_B or k_F . This immediately gives pressure,

$$P = \rho_B^2 \frac{\partial}{\partial \rho_B} \left(\frac{\mathcal{E}}{\rho_B} \right).\tag{5}$$

Thermodynamic stability of the matter in the liquid phase is stated as $\partial P / \partial \rho_B > 0$. Since the ratio of the sound velocity c_s to the light velocity c is given by

$$\frac{c_s}{c} = \sqrt{\frac{1}{M} \frac{\partial P}{\partial \rho_B}},\tag{6}$$

$(c_s/c)^2 < 0$ in Fig.1 indicates the existence of a mechanical instability to the gas phase. In this paper we adopt $M = 939$ MeV, $m_\sigma = 550$ MeV, $m_\omega = 783$ MeV, $g_\sigma^2 = 91.64$, and $g_\omega^2 = 136.2$ [32].

Quantum mechanically, stability of a state is determined by the second variation of the energy with respect to the fields [28]. This is equivalent to the random phase approximation (RPA). The RPA in the present model in which the nucleon-nucleon interaction is mediated by mesons is formulated by calculating the meson propagators that couple to the particle-hole and particle-antiparticle polarizations [6, 29, 30]. The Dyson equation that determines

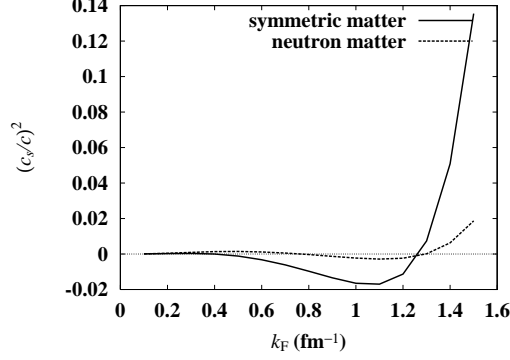


FIG. 1: Squared ratios of the sound velocity to the light velocity as a function of the Fermi momentum.

the RPA propagator D is given by

$$D = D_0 + D_0 \Pi D \quad (7)$$

(pictorially given in Fig.2), where the lowest order propagator,

$$D_0 = \begin{pmatrix} D_0^S & 0 \\ 0 & D_{0\mu\nu}^V \end{pmatrix}, \quad (8)$$

and the polarization insertion,

$$\Pi = \begin{pmatrix} \Pi^S & \Pi_\nu^M \\ \Pi_\mu^M & \Pi_{\mu\nu}^V \end{pmatrix}, \quad (9)$$

are given by 5×5 matrices. Their components are specified as

$$D_0^S(q) = \frac{1}{q^2 - m_\sigma^2 + i\epsilon},$$

$$D_{0\mu\nu}^V(q) = \left(g_{\mu\nu} - \frac{q_\mu q_\nu}{m_\omega^2} \right) D_0^V(q), \quad D_0^V(q) = \frac{-1}{q^2 - m_\omega^2 + i\epsilon}, \quad (10)$$

and

$$\begin{aligned} \Pi^S(q) &= -ig_\sigma^2 \int \frac{d^4k}{(2\pi)^4} \text{Tr}[G(k)G(k+q)], \\ \Pi_{\mu\nu}^V(q) &= -ig_\omega^2 \int \frac{d^4k}{(2\pi)^4} \text{Tr}[\gamma_\mu G(k)\gamma_\nu G(k+q)], \\ \Pi_\mu^M(q) &= ig_\sigma g_\omega \int \frac{d^4k}{(2\pi)^4} \text{Tr}[\gamma_\mu G(k)G(k+q)]. \end{aligned} \quad (11)$$

Here $G(k)$ stands for the nucleon propagator and the Tr symbol includes isospin. Π_μ^M stands for the matter induced σ - ω mixed polarization; a σ excites a particle-hole pair and then it

decays into an ω and vice versa. Since Eq.(7) is formally solved as

$$D = \frac{1}{1 - D_0 \Pi} D_0, \quad (12)$$

zeros of the dielectric function,

$$\epsilon = \det(1 - D_0 \Pi) \quad (13)$$

determines collective excitations.

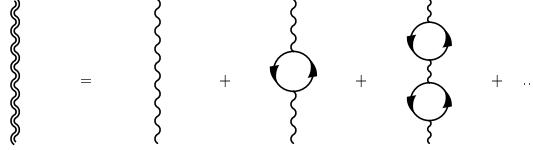


FIG. 2: Feynman diagram representing the RPA meson propagator.

For the present purpose, investigating instability, only the real parts at zero energy transfer are necessary. Therefore we set

$$\begin{aligned} D_0^S &= \frac{-1}{|\mathbf{q}|^2 + m_\sigma^2}, \\ D_0^V &= \frac{1}{|\mathbf{q}|^2 + m_\omega^2}, \end{aligned} \quad (14)$$

and the second term in $D_{0\mu\nu}^V$ drops because of the baryon number conservation. This conservation law also restricts non-vanishing components among Π ; if we choose the coordinate system as $q = (q^0, 0, 0, |\mathbf{q}|)$, only $\Pi^L \equiv \Pi_{00}^V - \Pi_{33}^V$ and $\Pi^T \equiv \Pi_{11}^V = \Pi_{22}^V$ among $\Pi_{\mu\nu}^V$ and $\Pi^0 \equiv \Pi_\mu^M$ among Π_μ^M survive. Note that energy transfer q^0 is set to zero, that is the instantaneous approximation. After some permutations, $1 - D_0 \Pi$ becomes block diagonal, and consequently the dielectric function reduces to

$$\begin{aligned} \epsilon &= \epsilon_L \epsilon_T^2, \\ \epsilon_L &= (1 - D_0^S \Pi^S)(1 - D_0^V \Pi^L) - D_0^S D_0^V (\Pi^0)^2, \\ \epsilon_T &= 1 + D_0^V \Pi^T. \end{aligned} \quad (15)$$

The transverse dielectric function ϵ_T is always positive in the density region in which superfluidity is realized, whereas the longitudinal one ϵ_L becomes negative at intermediate densities; this represents the liquid-gas instability.

In this work, we concentrate on the particle-hole polarization. We examine two ways to extract the particle-hole polarization; (1) the standard Feynman-density (FD) decomposition

of $G(k)$ and (2) the particle-hole-antiparticle (pha) decomposition. From its definition, the nucleon propagator in the medium is given by

$$\begin{aligned}
G(k) &= \frac{1}{2E^*(k)} \left[(\gamma_\mu K^\mu + M^*) \left(\frac{1 - \theta(k_F - |\mathbf{k}|)}{k^0 - E^*(k) + i\epsilon} + \frac{\theta(k_F - |\mathbf{k}|)}{k^0 - E^*(k) - i\epsilon} \right) \right. \\
&\quad \left. - (\gamma_\mu \tilde{K}^\mu + M^*) \frac{1}{k^0 + E^*(k) - i\epsilon} \right] \\
&\equiv G_p(k) + G_h(k) + G_a(k),
\end{aligned} \tag{16}$$

where

$$\begin{aligned}
K &= (E^*(k), \mathbf{k}), \quad \tilde{K} = (-E^*(k), \mathbf{k}), \\
E^*(k) &= \sqrt{\mathbf{k}^2 + M^{*2}}.
\end{aligned} \tag{17}$$

The first, the second, and the third terms represent the propagator of particle, hole, and antiparticle, respectively. By sorting them with respect to the Heaviside function, another form,

$$\begin{aligned}
G(k) &= (\gamma_\mu k^\mu + M^*) \left(\frac{1}{k^2 - M^{*2} + i\epsilon} + \frac{i\pi}{E^*(k)} \delta(k^0 - E^*(k)) \theta(k_F - |\mathbf{k}|) \right) \\
&\equiv G_F(k) + G_D(k),
\end{aligned} \tag{18}$$

is obtained. The first and the second terms are called the Feynman and the density parts, respectively. The former consists of the antiparticle propagation and a part of the particle propagation, while the latter consists of the hole propagation and the other part of the particle propagation. In the standard FD decomposition, the density dependent $G_F G_D + G_D G_F$ part in Eq.(11) is regarded as the particle-hole polarization. Note that the $G_D G_D$ part is pure imaginary and therefore is not necessary for the present purpose. In the pha decomposition, the $G_p G_h + G_h G_p$ part in Eq.(11) represents the particle-hole polarization and this directly corresponds to that in non-relativistic calculations [33]. The concrete expressions of Π are given in Appendix A.

Figure 3 shows the longitudinal dielectric function ϵ_L of the FD and the pha cases for symmetric nuclear matter. At low momentum transfers, ϵ_L becomes negative in both cases. The density range of the instability coincides very well with Fig. 1 in the FD case. This is consistent with Ref. [28] in which the density range of the instability hardly changes even after inclusion of the vacuum polarization. In the pha case the instability region shrinks. These results indicate that the liquid-gas instability occurred in a wide density range affects

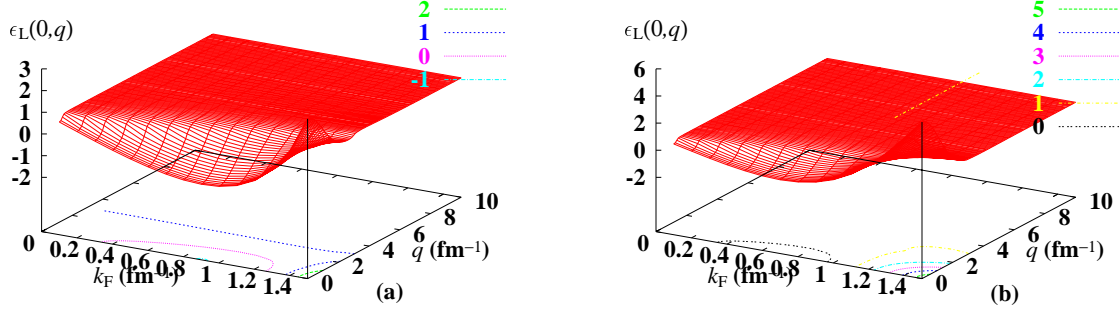


FIG. 3: (Color online) Longitudinal dielectric functions for symmetric nuclear matter as a function of the Fermi momentum and the momentum transfer, (a) the FD case, (b) the pha case.

the pairing properties that are calculated by using the RPA meson propagator that exhibits instability.

III. MEDIUM POLARIZATION EFFECTS ON SUPERFLUIDITY

The concrete form of the RPA meson propagator is given by

$$D = \frac{1}{1 - D_0 \Pi} D_0 = \begin{pmatrix} \frac{(1 - D_0^V \Pi^L) D_0^S}{\epsilon_L} & \frac{D_0^S D_0^V \Pi^0}{\epsilon_L} & 0 & 0 & 0 \\ \frac{D_0^V D_0^S \Pi^0}{\epsilon_L} & \frac{(1 - D_0^S \Pi^S) D_0^V}{\epsilon_L} & 0 & 0 & 0 \\ 0 & 0 & \frac{-D_0^V}{\epsilon_T} & 0 & 0 \\ 0 & 0 & 0 & \frac{-D_0^V}{\epsilon_T} & 0 \\ 0 & 0 & 0 & 0 & -D_0^V \end{pmatrix}. \quad (19)$$

This gives the particle-particle channel interaction that determines superfluidity as

$$V_{\text{RPA}} = \sum_{a,b} g_a \Gamma_a D^{a,b} g_b \Gamma_b, \\ g_a = \begin{cases} g_\sigma \\ -g_\omega \end{cases}, \quad \Gamma_a = \begin{cases} 1 : a = -1 \\ \gamma_\mu : a = \mu \end{cases}. \quad (20)$$

The antisymmetrized matrix element of this interaction for the 1S_0 pairing channel is given by

$$\bar{v}(\mathbf{p}, \mathbf{k}) = \langle \mathbf{p}s', \tilde{\mathbf{p}}s' | V_{\text{RPA}} | \mathbf{k}s, \tilde{\mathbf{k}}s \rangle - \langle \mathbf{p}s', \tilde{\mathbf{p}}s' | V_{\text{RPA}} | \tilde{\mathbf{k}}s, \mathbf{k}s \rangle, \quad (21)$$

here the argument $|\mathbf{q}|$ of D in V_{RPA} is specified as $\mathbf{q} = \mathbf{p} - \mathbf{k}$, and tildes represent time reversal. Since, by ignoring the coupling to the negative-energy states, the relativistic Nambu-Gor'kov formalism reduces to the usual gap equation [34, 35],

$$\Delta(p) = -\frac{1}{8\pi^2} \int_0^\infty \bar{v}(p, k) \frac{\Delta(k)}{\sqrt{(E_k - E_{\text{F}})^2 + \Delta^2(k)}} k^2 dk, \quad (22)$$

after an integration with respect to the angle between \mathbf{p} and \mathbf{k} . The effective mass equation (3) is slightly modified when superfluidity sets in as

$$M^* = M - \frac{g_\sigma^2}{m_\sigma^2} \frac{\lambda}{\pi^2} \int_0^\infty \frac{M^*}{\sqrt{k^2 + M^{*2}}} v_k^2 k^2 dk, \\ v_k^2 = \frac{1}{2} \left(1 - \frac{E_k - E_{\text{F}}}{\sqrt{(E_k - E_{\text{F}})^2 + \Delta^2(k)}} \right). \quad (23)$$

Here $E_k = E^*(k) + g_\omega \langle \omega_0 \rangle$. Using these equations we calculate superfluidity in nuclear matter assuming that it is in the liquid phase even at the density range in which the liquid-gas instability would occur, as usual. We set the upper bound of the integrations as 20 fm^{-1} .

Here, some discussion about our choice of the interaction is in order. In the lowest order (the tree level; $D \rightarrow D_0$), V_{RPA} reduces to the one boson exchange (OBE) interaction V_{OBE} given by the RMF vertices (see Fig.2). It has been well known that this OBE interaction gives unphysically large pairing gap [34]. Its reason can be traced back to the fact that the RMF vertices were tuned only below the Fermi momentum. In order to discuss the higher order (polarization) effects this OBE result must be improved beforehand. We accomplish this by introducing a form factor that modulates the high momentum part of the interaction smoothly [36] as follows. Note that the authors of Ref. [26] adopted sudden momentum cutoffs so as to reproduce the virtual state in the T matrix. We argued in Ref. [36] that the sudden cutoff distorts the shape of the short range pair wave function. See also Ref. [37] for the sudden momentum cutoff that reproduces the results of a bare interaction in the pairing calculation. From a general argument, the lowest order in the particle-particle channel interaction that gives pairing should be a bare interaction and the particle-hole channel interaction that determines the medium polarization should be an in-medium one in principle. In the present investigation, however, we calculate both the tree and the bubble contributions on the same footing adopting an interaction of in-medium nature, which reproduces the results of a bare interaction in the tree level. That is, we regard, in a sense, the present

RMF-OBE interaction with a form factor resembles the Gogny force in the non-relativistic pairing calculations.

In order to modulate the high momentum interaction that enters into the pairing calculation, we introduce a form factor,

$$f(\mathbf{q}^2) = \frac{\Lambda^2}{\Lambda^2 + \mathbf{q}^2}, \quad (24)$$

at each vertex. This does not affect the mean field (Hartree) part with the momentum transfer $\mathbf{q} = 0$. The parameter Λ is determined so as to minimize the difference in the pairing properties from the results of the RMF+Bonn calculation, that is, a hybrid calculation performed by adopting single particle states from the RMF model and the Bonn potential as the pairing interaction. Here we adopt the Bonn-B potential because this has a moderate property among the available (charge-independent) versions A, B, and C [38]. The pair wave function,

$$\begin{aligned} \phi(k) &= \frac{1}{2} \frac{\Delta(k)}{E_{\text{qp}}(k)}, \\ E_{\text{qp}}(k) &= \sqrt{(E_k - E_{k_F})^2 + \Delta^2(k)}, \end{aligned} \quad (25)$$

is related to the gap at the Fermi surface,

$$\Delta(k_F) = -\frac{1}{4\pi^2} \int_0^\infty \bar{v}(k_F, k) \phi(k) k^2 dk, \quad (26)$$

and its derivative determines the coherence length,

$$\xi = \left(\frac{\int_0^\infty \left| \frac{d\phi}{dk} \right|^2 k^2 dk}{\int_0^\infty |\phi|^2 k^2 dk} \right)^{\frac{1}{2}}, \quad (27)$$

which measures the spatial size of the Cooper pairs. These expressions indicate that $\Delta(k_F)$ and ξ carry independent information, ϕ and $\frac{d\phi}{dk}$, respectively, in strongly-coupled systems, whereas they are intimately related to each other in weakly-coupled ones. Therefore we search for Λ that minimizes

$$\chi^2 = \frac{1}{2N} \sum_{k_F} \left\{ \left(\frac{\Delta(k_F)_{\text{RMF}} - \Delta(k_F)_{\text{Bonn}}}{\Delta(k_F)_{\text{Bonn}}} \right)^2 + \left(\frac{\xi_{\text{RMF}} - \xi_{\text{Bonn}}}{\xi_{\text{Bonn}}} \right)^2 \right\}, \quad (28)$$

with $N = 11$ ($k_F = 0.2, 0.3, \dots, 1.2 \text{ fm}^{-1}$). The obtained value is $\Lambda = 7.26 \text{ fm}^{-1}$ [36]. For consistency we included the form factor also in the polarization diagrams but it almost would not affect them because the polarization affects only low momenta (see following figures).

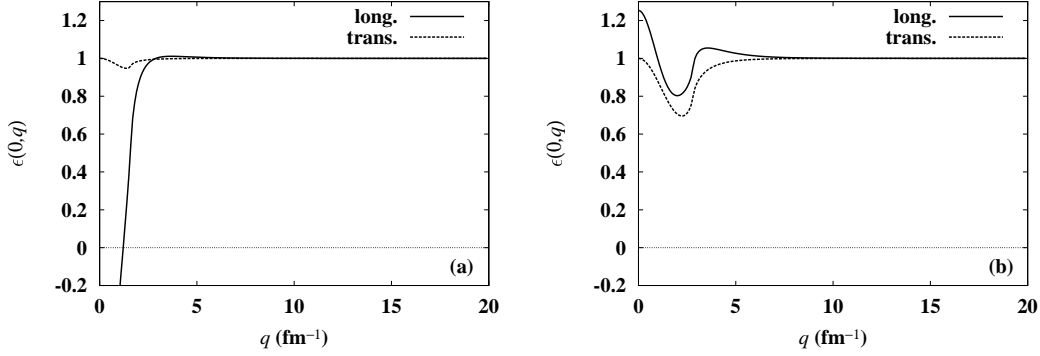


FIG. 4: Cross sections of the dielectric functions for the FD case of symmetric nuclear matter as a function of the momentum transfer, (a) $k_F = 0.8 \text{ fm}^{-1}$, (b) $k_F = 1.4 \text{ fm}^{-1}$.

Equation (19) indicates that V_{RPA} becomes ill-defined when the liquid-gas instability occurs. This means that superfluidity in the liquid-gas coexistent phase rather than that in the liquid phase should be considered. However, in the present calculation, we consider the case in which the system stays in the liquid phase also in the instability region ($0.3 \text{ fm}^{-1} < k_F < 1.3 \text{ fm}^{-1}$ in the FD case) as usual. Therefore in that region only qualitative discussion is possible. Reference [27] also mentioned the existence of the instability. Note that discussion is quantitative in high and low density regions that are free from the instability. Figure 4 shows the cross sections of the longitudinal and the transverse dielectric functions. Figure 4(a) is for $k_F = 0.8 \text{ fm}^{-1}$ and (b) is for $k_F = 1.4 \text{ fm}^{-1}$. The former indicates that a low momentum cutoff is necessary to regularize the calculation for the instability region. Thus, we introduce ϵ_{cut} that operates to cut $|\mathbf{q}|$ for which $\epsilon_{\text{L/T}}(0, |\mathbf{q}|) \leq \epsilon_{\text{cut}}$. Since other parameters were determined at the saturation density, we chose $\epsilon_{\text{cut}} = 0.65$ that maintains the full variation of ϵ_{L} and ϵ_{T} around this density (see Fig.4(b)). This also serves to make the k_F -dependence of $\Delta(k_F)$ smooth at the boundary of the instability region. Figure 5 reports the dependence of $\Delta(k_F = 0.8 \text{ fm}^{-1})$ on ϵ_{cut} . Its dependence is moderate around the chosen value. Figure 6 compares $\Delta(k_F)$. This figure shows that the medium polarization increases the gap at all densities in the FD case. This is common to the previous calculation [31] in which the form factor to modulate the high momentum interaction was not introduced. Batista et al. [26] who weakened the effect of the bubble diagram by their x parameter obtained a similar result. The contents of the polarization interaction, $V_{\text{RPA}} - V_{\text{OBE}}$, are decomposed in Fig. 7. (The k -dependence in Fig. 7(a) is a result of ϵ_{cut} for q .) These figures

represent a characteristic feature that the σ polarization and the longitudinal ω polarization give strong attractions whereas the σ - ω mixed polarization gives a strong repulsion and they strongly cancel each other. Remaining tiny attraction leads to the increase of $\Delta(k_F)$. From this viewpoint, the neglect of the σ - ω mixed polarization in Ref. [25] would cause an imbalance. The transverse ω polarization that represents the spin density fluctuation is slightly repulsive, but the repulsion in the momentum region in which $\Delta(k) < 0$ (that is predominantly determined by V_{OBE}) also increases $\Delta(k_F)$ because of the structure of the gap equation (22).

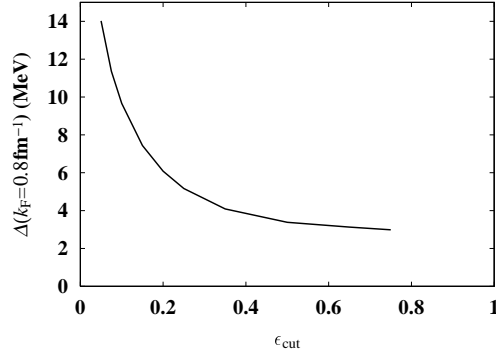


FIG. 5: Cutoff parameter dependence of $\Delta(k_F)$ at $k_F = 0.8 \text{ fm}^{-1}$.

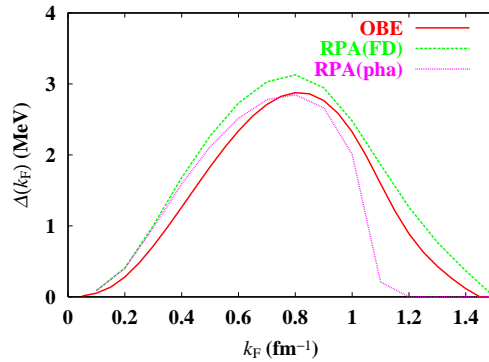


FIG. 6: (Color online) Pairing gaps at the Fermi surface for symmetric nuclear matter as a function of the Fermi momentum.

Figure 6 also reports the pha case. The results of the FD and the pha cases are very close to each other at low densities. This is because the particle propagation contained G_D is small. However, their difference grows as density increases; at high k_F the polarization reduces $\Delta(k_F)$ in contrast to the FD case. This is brought about by the behavior that the

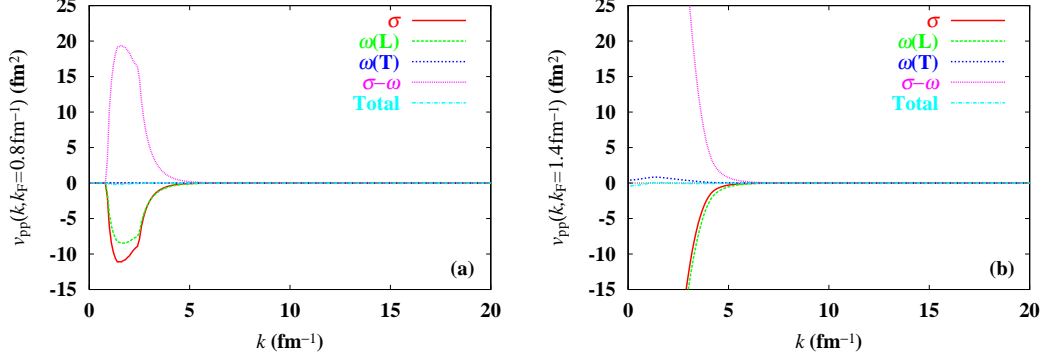


FIG. 7: (Color online) Decomposition of the polarization interaction for the FD case of symmetric nuclear matter as a function of the momentum, (a) $k_F = 0.8 \text{ fm}^{-1}$, (b) $k_F = 1.4 \text{ fm}^{-1}$.

total polarization interaction becomes repulsive (Fig. 8).

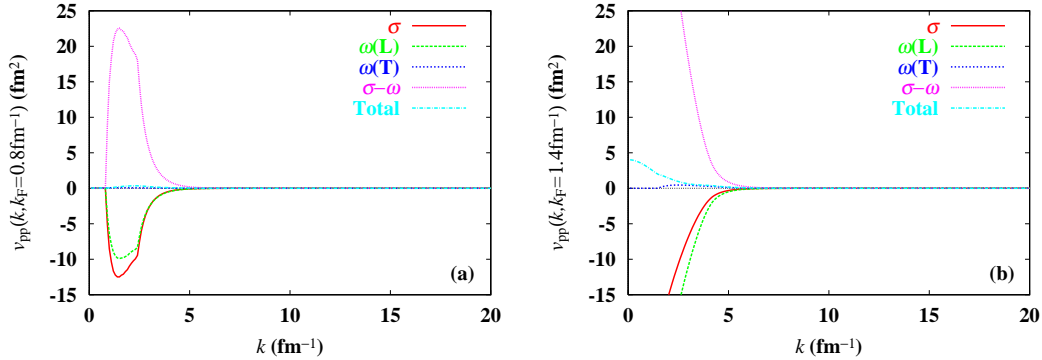


FIG. 8: (Color online) The same as Fig. 7 but for the pha case.

Finally we briefly mention the pure neutron matter case. It is subtle whether liquid-gas instability occurs in pure neutron matter or not. In the present calculations it occurs in the FD case (Fig. 9(a)). In the pha case it does not occur but ϵ_L strongly decreases at medium k_F (Fig. 9(b)). Consequently the behavior of $\Delta(k_F)$ is similar to the symmetric matter case (Fig. 10).

IV. DISCUSSION AND CONCLUSION

In symmetric nuclear matter, the RPA leads to liquid-gas instability at moderate densities even at zero temperature. In the present study, we concentrated on the medium polarization, but Ref. [28] showed that liquid-gas instability survives even after inclusion of the vacuum

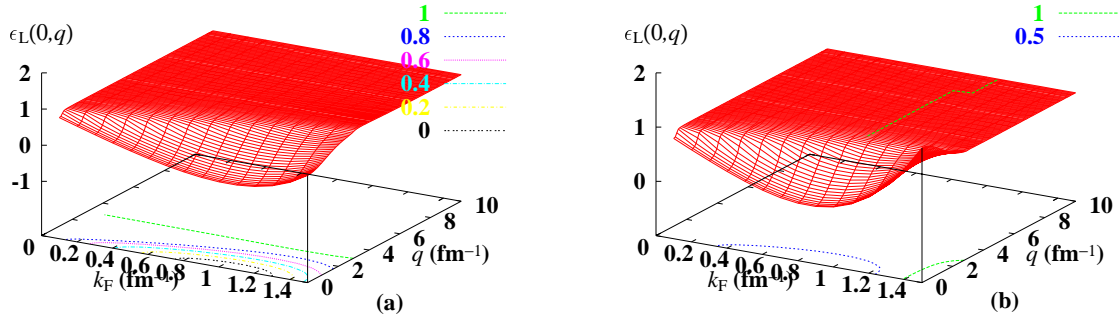


FIG. 9: (Color online) The same as Fig. 3 but for pure neutron matter.

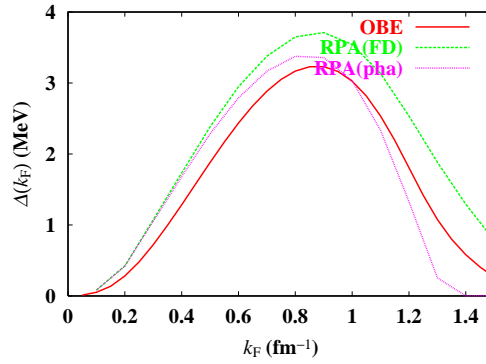


FIG. 10: (Color online) The same as Fig. 6 but for pure neutron matter.

polarization. This indicates that the medium polarization effects on superfluidity should be considered in the liquid-gas coexistent phase rather than in the liquid phase. In the present investigation, however, we have studied superfluidity in the liquid phase, as usual. Therefore only qualitative discussion is allowed for the density region in which the instability occurs; the gap increases from the OBE result. In other regions free from the instability, a quantitative discussion is possible; the gap increases in the FD decomposition whereas decreases in the pha decomposition at high densities. At low densities the gap increases in both cases. These results are brought about by the characteristic cancellation between the attraction from the σ polarization and the longitudinal ω polarization and the repulsion from the σ - ω mixed polarization. The result for the FD case is consistent with that of another relativistic study in Ref. [26] and of a non-relativistic study in Ref. [27]. Both cases are consistent with Ref. [19]. It is known that the coupling to surface vibrations enhances

pairing in finite nuclei [39, 40, 41]. This tendency is in the same direction as the FD case in the present calculation. But, since the polarization in the matter case is density modes, their mutual correspondence should be clarified.

It is a subtle problem whether liquid-gas instability occurs in pure neutron matter or not. In the present calculation, it occurs in the FD case. Although it does not occur in the pha case, the longitudinal dielectric function decreases strongly. Consequently the results for the gap are similar to the symmetric matter case. Note that the decrease of the Landau parameter F_0 to around -1 was reported in Ref. [27]. In most of non-relativistic calculations [14, 15, 16, 17, 18, 19, 20, 21, 22], decrease of the gap was reported. This is due to non-occurrence of liquid-gas instability and to the repulsive effect of the spin density fluctuation. In the present model, the effect of the transverse ω polarization that corresponds to the spin density mode is weak. It is worth noting here that a recent ab initio calculation [23] concluded that the polarization effect in pure neutron matter is weak.

It should be stressed that it is an approximation to consider only the medium (particle-hole) polarization in the relativistic model; the vacuum (particle-antiparticle) polarization should also be included. Since the gap is sensitive to the tiny remnant of the strong cancellation mentioned above, future inclusion of the vacuum polarization would be important. This will be studied separately. According to Refs. [42, 43], the vacuum polarization leads to vector meson mass decrease. In a previous paper [44] we examined this meson mass decrease using the in-medium Bonn potential and concluded that it reduces the gap.

Other ingredients that are not considered in the present study are inclusion of exchange of other mesons like π and ρ , and the selfenergy effects [45, 46, 47]. Study of superfluidity in the liquid-gas coexistent phase is also an interesting issue.

Acknowledgments

The author acknowledges Professor P. Ring for suggesting the problem and Professor H. Kouno for useful discussions.

APPENDIX A: MEDIUM POLARIZATION INSERTIONS

1. Feynman-density decomposition

$$\begin{aligned}\Pi^S = & \frac{2\lambda g_\sigma^2}{(2\pi)^2} \left[k_F E_F^* - \frac{1}{2} (6M^{*2} + |\mathbf{q}|^2) \ln \left(\frac{k_F + E_F^*}{M^*} \right) \right. \\ & + \frac{4M^{*2} + |\mathbf{q}|^2}{4|\mathbf{q}|} \left(2E_F^* - \sqrt{4M^{*2} + |\mathbf{q}|^2} \right) \ln \left| \frac{|\mathbf{q}| - 2k_F}{|\mathbf{q}| + 2k_F} \right| \\ & \left. + \frac{(4M^{*2} + |\mathbf{q}|^2)^{3/2}}{4|\mathbf{q}|} \ln \left| \frac{E_F^* \sqrt{4M^{*2} + |\mathbf{q}|^2} + 2M^{*2} + |\mathbf{q}| k_F}{E_F^* \sqrt{4M^{*2} + |\mathbf{q}|^2} + 2M^{*2} - |\mathbf{q}| k_F} \right| \right].\end{aligned}\quad (\text{A1})$$

$$\begin{aligned}\Pi^L = & -\frac{2\lambda g_\omega^2}{(2\pi)^2} \left[\frac{4}{3} k_F E_F^* - \frac{1}{3} |\mathbf{q}|^2 \ln \left(\frac{k_F + E_F^*}{M^*} \right) \right. \\ & + \frac{1}{6|\mathbf{q}|} \left(E_F^* (3|\mathbf{q}|^2 - 4E_F^{*2}) + (2M^{*2} - |\mathbf{q}|^2) \sqrt{4M^{*2} + |\mathbf{q}|^2} \right) \ln \left| \frac{|\mathbf{q}| - 2k_F}{|\mathbf{q}| + 2k_F} \right| \\ & \left. - \frac{1}{6|\mathbf{q}|} (2M^{*2} - |\mathbf{q}|^2) \sqrt{4M^{*2} + |\mathbf{q}|^2} \ln \left| \frac{E_F^* \sqrt{4M^{*2} + |\mathbf{q}|^2} + 2M^{*2} + |\mathbf{q}| k_F}{E_F^* \sqrt{4M^{*2} + |\mathbf{q}|^2} + 2M^{*2} - |\mathbf{q}| k_F} \right| \right].\end{aligned}\quad (\text{A2})$$

$$\begin{aligned}\Pi^T = & -\frac{2\lambda g_\omega^2}{(2\pi)^2} \left[-\frac{1}{3} k_F E_F^* + \frac{1}{3} |\mathbf{q}|^2 \ln \left(\frac{k_F + E_F^*}{M^*} \right) \right. \\ & - \frac{1}{6|\mathbf{q}|} \left(E_F^* (2E_F^{*2} - 6M^{*2} + \frac{3}{2} |\mathbf{q}|^2) + (2M^{*2} - |\mathbf{q}|^2) \sqrt{4M^{*2} + |\mathbf{q}|^2} \right) \ln \left| \frac{|\mathbf{q}| - 2k_F}{|\mathbf{q}| + 2k_F} \right| \\ & \left. + \frac{1}{6|\mathbf{q}|} (2M^{*2} - |\mathbf{q}|^2) \sqrt{4M^{*2} + |\mathbf{q}|^2} \ln \left| \frac{E_F^* \sqrt{4M^{*2} + |\mathbf{q}|^2} + 2M^{*2} + |\mathbf{q}| k_F}{E_F^* \sqrt{4M^{*2} + |\mathbf{q}|^2} + 2M^{*2} - |\mathbf{q}| k_F} \right| \right].\end{aligned}\quad (\text{A3})$$

$$\Pi^0 = \frac{2\lambda g_\sigma g_\omega}{(2\pi)^2} M^* \left[k_F + \frac{|\mathbf{q}|^2 - 4k_F^2}{4|\mathbf{q}|} \ln \left| \frac{|\mathbf{q}| - 2k_F}{|\mathbf{q}| + 2k_F} \right| \right].\quad (\text{A4})$$

2. Particle-hole-antiparticle decomposition

$$\begin{aligned}
\Pi^S = & \frac{2\lambda g_\sigma^2}{(2\pi)^2} \left[\frac{1}{2} k_F E_F^* - \frac{1}{4} (6M^{*2} + |\mathbf{q}|^2) \ln \left(\frac{k_F + E_F^*}{M^*} \right) \right. \\
& - \frac{(4M^{*2} + |\mathbf{q}|^2)^{3/2}}{8|\mathbf{q}|} \left(2 \ln \left| \frac{|\mathbf{q}| - 2k_F}{|\mathbf{q}| + 2k_F} \right| - \ln \left| \frac{E_F^* \sqrt{4M^{*2} + |\mathbf{q}|^2} + 2M^{*2} + |\mathbf{q}|k_F}{E_F^* \sqrt{4M^{*2} + |\mathbf{q}|^2} + 2M^{*2} - |\mathbf{q}|k_F} \right| \right. \\
& + \ln \left| \frac{\sqrt{(k_F + |\mathbf{q}|)^2 + M^{*2}} \sqrt{4M^{*2} + |\mathbf{q}|^2} + 2M^{*2} + |\mathbf{q}|^2 + |\mathbf{q}|k_F}{\sqrt{(k_F - |\mathbf{q}|)^2 + M^{*2}} \sqrt{4M^{*2} + |\mathbf{q}|^2} + 2M^{*2} + |\mathbf{q}|^2 - |\mathbf{q}|k_F} \right| \Big) \\
& - \frac{1}{6|\mathbf{q}|} \left(((k_F + |\mathbf{q}|)^2 + M^{*2})^{3/2} - ((k_F - |\mathbf{q}|)^2 + M^{*2})^{3/2} \right) \\
& + \frac{1}{4} k_F \left(\sqrt{(k_F + |\mathbf{q}|)^2 + M^{*2}} + \sqrt{(k_F - |\mathbf{q}|)^2 + M^{*2}} \right) \\
& - \frac{M^{*2}}{|\mathbf{q}|} \left(\sqrt{(k_F + |\mathbf{q}|)^2 + M^{*2}} - \sqrt{(k_F - |\mathbf{q}|)^2 + M^{*2}} \right) \\
& - \frac{E_F^*}{2|\mathbf{q}|} (4M^{*2} + |\mathbf{q}|^2) \ln \left| \frac{\sqrt{(k_F + |\mathbf{q}|)^2 + M^{*2}} - E_F^*}{\sqrt{(k_F - |\mathbf{q}|)^2 + M^{*2}} - E_F^*} \right| \\
& + \frac{1}{8} (6M^{*2} + |\mathbf{q}|^2) \ln \left| \frac{(\sqrt{(k_F + |\mathbf{q}|)^2 + M^{*2}} + k_F + |\mathbf{q}|)(\sqrt{(k_F - |\mathbf{q}|)^2 + M^{*2}} + k_F - |\mathbf{q}|)}{M^{*2}} \right| \Big].
\end{aligned} \tag{A5}$$

$$\begin{aligned}
\Pi^L = & -\frac{2\lambda g_\omega^2}{(2\pi)^2} \left[\frac{2}{3} k_F E_F^* - \frac{1}{6} |\mathbf{q}|^2 \ln \left(\frac{k_F + E_F^*}{M^*} \right) \right. \\
& + \frac{1}{12|\mathbf{q}|} (2M^{*2} - |\mathbf{q}|^2) \sqrt{4M^{*2} + |\mathbf{q}|^2} \left(2 \ln \left| \frac{|\mathbf{q}| - 2k_F}{|\mathbf{q}| + 2k_F} \right| - \ln \left| \frac{E_F^* \sqrt{4M^{*2} + |\mathbf{q}|^2} + 2M^{*2} + |\mathbf{q}|k_F}{E_F^* \sqrt{4M^{*2} + |\mathbf{q}|^2} + 2M^{*2} - |\mathbf{q}|k_F} \right| \right. \\
& \left. \left. + \ln \left| \frac{\sqrt{(k_F + |\mathbf{q}|)^2 + M^{*2}} \sqrt{4M^{*2} + |\mathbf{q}|^2} + 2M^{*2} + |\mathbf{q}|^2 + |\mathbf{q}|k_F}{\sqrt{(k_F - |\mathbf{q}|)^2 + M^{*2}} \sqrt{4M^{*2} + |\mathbf{q}|^2} + 2M^{*2} + |\mathbf{q}|^2 - |\mathbf{q}|k_F} \right| \right) \right. \\
& + \frac{1}{15|\mathbf{q}|^3} \left(((k_F + |\mathbf{q}|)^2 + M^{*2})^{5/2} - ((k_F - |\mathbf{q}|)^2 + M^{*2})^{5/2} \right) \\
& - \frac{k_F}{3|\mathbf{q}|^2} \left(((k_F + |\mathbf{q}|)^2 + M^{*2})^{3/2} + ((k_F - |\mathbf{q}|)^2 + M^{*2})^{3/2} \right) \\
& + \frac{11}{18|\mathbf{q}|} \left(((k_F + |\mathbf{q}|)^2 + M^{*2})^{3/2} - ((k_F - |\mathbf{q}|)^2 + M^{*2})^{3/2} \right) \\
& - \frac{7}{6} k_F \left(\sqrt{(k_F + |\mathbf{q}|)^2 + M^{*2}} + \sqrt{(k_F - |\mathbf{q}|)^2 + M^{*2}} \right) \\
& - \frac{2M^{*2} + 5|\mathbf{q}|^2}{6|\mathbf{q}|} \left(\sqrt{(k_F + |\mathbf{q}|)^2 + M^{*2}} - \sqrt{(k_F - |\mathbf{q}|)^2 + M^{*2}} \right) \\
& + \frac{E_F^*}{6|\mathbf{q}|} (4E_F^{*2} - 3|\mathbf{q}|^2) \ln \left| \frac{\sqrt{(k_F + |\mathbf{q}|)^2 + M^{*2}} - E_F^*}{\sqrt{(k_F - |\mathbf{q}|)^2 + M^{*2}} - E_F^*} \right| \\
& \left. + \frac{1}{12} |\mathbf{q}|^2 \ln \left| \frac{(\sqrt{(k_F + |\mathbf{q}|)^2 + M^{*2}} + k_F + |\mathbf{q}|)(\sqrt{(k_F - |\mathbf{q}|)^2 + M^{*2}} + k_F - |\mathbf{q}|)}{M^{*2}} \right| \right]. \quad (\text{A6})
\end{aligned}$$

$$\begin{aligned}
\Pi^T = & -\frac{2\lambda g_\omega^2}{(2\pi)^2} \left[-\frac{1}{6}k_F E_F^* + \frac{1}{6}|\mathbf{q}|^2 \ln \left(\frac{k_F + E_F^*}{M^{*2}} \right) \right. \\
& -\frac{1}{12|\mathbf{q}|} (2M^{*2} - |\mathbf{q}|^2) \sqrt{4M^{*2} + |\mathbf{q}|^2} \left(2 \ln \left| \frac{|\mathbf{q}| - 2k_F}{|\mathbf{q}| + 2k_F} \right| - \ln \left| \frac{E_F^* \sqrt{4M^{*2} + |\mathbf{q}|^2} + 2M^{*2} + |\mathbf{q}|k_F}{E_F^* \sqrt{4M^{*2} + |\mathbf{q}|^2} + 2M^{*2} - |\mathbf{q}|k_F} \right| \right. \\
& + \ln \left| \frac{\sqrt{(k_F + |\mathbf{q}|)^2 + M^{*2}} \sqrt{4M^{*2} + |\mathbf{q}|^2} + 2M^{*2} + |\mathbf{q}|^2 + |\mathbf{q}|k_F}{\sqrt{(k_F - |\mathbf{q}|)^2 + M^{*2}} \sqrt{4M^{*2} + |\mathbf{q}|^2} + 2M^{*2} + |\mathbf{q}|^2 - |\mathbf{q}|k_F} \right| \Big) \\
& + \frac{1}{30|\mathbf{q}|^3} \left(((k_F + |\mathbf{q}|)^2 + M^{*2})^{5/2} - ((k_F - |\mathbf{q}|)^2 + M^{*2})^{5/2} \right) \\
& - \frac{k_F}{6|\mathbf{q}|^2} \left(((k_F + |\mathbf{q}|)^2 + M^{*2})^{3/2} + ((k_F - |\mathbf{q}|)^2 + M^{*2})^{3/2} \right) \\
& + \frac{17}{36|\mathbf{q}|} \left(((k_F + |\mathbf{q}|)^2 + M^{*2})^{3/2} - ((k_F - |\mathbf{q}|)^2 + M^{*2})^{3/2} \right) \\
& - \frac{5}{6}k_F \left(\sqrt{(k_F + |\mathbf{q}|)^2 + M^{*2}} + \sqrt{(k_F - |\mathbf{q}|)^2 + M^{*2}} \right) \\
& - \frac{8M^{*2} + 5|\mathbf{q}|^2}{12|\mathbf{q}|} \left(\sqrt{(k_F + |\mathbf{q}|)^2 + M^{*2}} - \sqrt{(k_F - |\mathbf{q}|)^2 + M^{*2}} \right) \\
& + \frac{E_F^*}{12|\mathbf{q}|} (4k_F^2 - 8M^{*2} + 3|\mathbf{q}|^2) \ln \left| \frac{\sqrt{(k_F + |\mathbf{q}|)^2 + M^{*2}} - E_F^*}{\sqrt{(k_F - |\mathbf{q}|)^2 + M^{*2}} - E_F^*} \right| \\
& \left. - \frac{1}{12}|\mathbf{q}|^2 \ln \left| \frac{(\sqrt{(k_F + |\mathbf{q}|)^2 + M^{*2}} + k_F + |\mathbf{q}|)(\sqrt{(k_F - |\mathbf{q}|)^2 + M^{*2}} + k_F - |\mathbf{q}|)}{M^{*2}} \right| \right]. \quad (\text{A7})
\end{aligned}$$

$$\begin{aligned}
\Pi^0 = & \frac{2\lambda g_\sigma g_\omega}{(2\pi)^2} M^* \left[\frac{1}{2}k_F - \frac{|\mathbf{q}|^2 - 4k_F^2}{4|\mathbf{q}|} \ln \left| \frac{\sqrt{(k_F + |\mathbf{q}|)^2 + M^{*2}} - E_F^*}{\sqrt{(k_F - |\mathbf{q}|)^2 + M^{*2}} - E_F^*} \right| \right. \\
& + \frac{3E_F^*}{4|\mathbf{q}|} \left(\sqrt{(k_F + |\mathbf{q}|)^2 + M^{*2}} - \sqrt{(k_F - |\mathbf{q}|)^2 + M^{*2}} \right) \\
& \left. + \frac{M^{*2}}{2|\mathbf{q}|} \ln \left| \frac{(\sqrt{(k_F + |\mathbf{q}|)^2 + M^{*2}} - E_F^* - |\mathbf{q}|)(\sqrt{(k_F + |\mathbf{q}|)^2 + M^{*2}} - E_F^* + |\mathbf{q}|)}{(\sqrt{(k_F - |\mathbf{q}|)^2 + M^{*2}} - E_F^* - |\mathbf{q}|)(\sqrt{(k_F - |\mathbf{q}|)^2 + M^{*2}} - E_F^* + |\mathbf{q}|)} \right| \right]. \quad (\text{A8})
\end{aligned}$$

-
- [1] T. Takatsuka and R. Tamagaki, Prog. Theor. Phys. Suppl. **112**, 27 (1993).
 - [2] H. -P. Duerr, Phys. Rev. **103**, 469 (1956).
 - [3] M. H. Jhonson and E. Teller, Phys. Rev. **98**, 783 (1955).
 - [4] S. A. Chin and J. D. Walecka, Phys. Lett. **B52**, 24 (1974).
 - [5] J. D. Walecka, Ann. Phys. **83**, 491 (1974).
 - [6] S. A. Chin, Ann. Phys. **108**, 301 (1977).

- [7] P. Ring, Prog. Part. Nucl. Phys. **37**, 193 (1996).
- [8] B. D. Serot and J. D. Walecka, Int. J. Mod. Phys. **E6**, 515 (1997).
- [9] A. B. Migdal, *Theory of Finite Fermi Systems and Applications to Atomic Nuclei* (Wiley, New York, 1967).
- [10] M. Baldo, J. Cugnon, A. Lejeune, and U. Lombardo, Nucl. Phys. **A515**, 409 (1990).
- [11] L. N. Cooper, R. L. Mills, and A. M. Sessler, Phys. Rev. **114**, 1377 (1959).
- [12] T. Marumori, T. Muroya, S. Takagi, H. Tanaka, and M. Yasuno, Prog. Theor. Phys. **25**, 1035 (1961).
- [13] G. F. Bertsch and H. Esbensen, Ann. Phys. **209**, 327 (1991).
- [14] J. W. Clark, C. -G. Källman, C. -H. Yang, and D. A. Chakkalakal, Phys. Lett. **B61**, 331 (1976).
- [15] J. M. C. Chen, J. W. Clark, E. Krotscheck, and R. A. Smith, Nucl. Phys. **A451**, 509 (1986).
- [16] T. L. Ainsworth, J. Wambach, and D. Pines, Phys. Lett. **B222**, 173 (1989).
- [17] J. Wambach, T. L. Ainsworth, and D. Pines, Nucl. Phys. **A555**, 128 (1993).
- [18] H. -J. Schulze, J. Cugnon, A. Lejeune, M. Baldo, and U. Lombardo, Phys. Lett. **B375**, 1 (1996).
- [19] H. Heiselberg, C. J. Pethick, H. Smith, and L. Viverit, Phys. Rev. Lett. **85**, 2418 (2000).
- [20] H. -J. Schulze, A. Polls, and A. Ramos, Phys. Rev. C **63**, 044310 (2001).
- [21] C. Shen, U. Lombardo, P. Schuck, W. Zuo, and N. Sandulescu, Phys. Rev. C **67**, 061302(R) (2003).
- [22] A. Schwenk, B. Friman, and G. E. Brown, Nucl. Phys. **A713**, 191 (2003).
- [23] A. Fabrocini, S. Fantoni, A. Yu. Illarionov, and K. A. Schmidt, Phys. Rev. Lett. **95**, 192501 (2005).
- [24] U. Lombardo, P. Schuck, and C. Shen, Nucl. Phys. **A731**, 392 (2004).
- [25] J. -S. Chen, P. -F. Zhuang, and J. -R. Li, Phys. Lett. **B585**, 85 (2004).
- [26] E. F. Batista, B. V. Carlson, and T. Frederico, Nucl. Phys. **A765**, 75 (2006).
- [27] C. Shen, U. Lombardo, and P. Schuck, Phys. Rev. C **71**, 054301 (2005).
- [28] B. L. Friman and P. A. Henning, Phys. Lett. **B206**, 579 (1988).
- [29] R. J. Furnstahl and C. J. Horowitz, Nucl. Phys. **A485**, 632 (1988).
- [30] K. Lim and C. J. Horowitz, Nucl. Phys. **A490**, 729 (1988).
- [31] M. Matsuzaki and P. Ring, in *Proc. APCTP Workshop on Astro-Hadron Physics in Honor*

- of Prof. Mannque Rho's 60th Birthday: Properties of Hadrons in Matter*, edited by G. E. Brown, C. -H. Lee, H. K. Lee, and D. -P. Min (World Scientific, Singapore, 1999), p. 243, nucl-th/9712060.
- [32] B. D. Serot and J. D. Walecka, *Adv. Nucl. Phys.* **16**, 1 (1986).
 - [33] N. Nakano, N. Noda, T. Mitsumori, K. Koide, H. Kouno, A. Hasegawa, and L. -G. Liu, *Phys. Rev. C* **56**, 3287 (1997).
 - [34] H. Kucharek and P. Ring, *Z. Phys.* **58**, 3407 (1998).
 - [35] M. Matsuzaki, *Phys. Rev. C* **58**, 3407 (1998).
 - [36] M. Matsuzaki and T. Tanigawa, *Nucl. Phys.* **A683**, 406 (2001).
 - [37] T. Tanigawa and M. Matsuzaki, *Prog. Theor. Phys.* **102**, 897 (1999).
 - [38] R. Machleidt, *Adv. Nucl. Phys.* **19**, 189 (1989).
 - [39] F. Barranco, R. A. Broglia, G. Gori, E. Vigezzi, P. F. Bortignon, and J. Terasaki, *Phys. Rev. Lett.* **83**, 2147 (1999).
 - [40] J. Terasaki, F. Barranco, R. A. Broglia, E. Vigezzi, and P. F. Bortignon, *Nucl. Phys.* **A697**, 127 (2002).
 - [41] G. Gori, F. Ramponi, F. Barranco, P. F. Bortignon, R. A. Broglia, G. Colò, and E. Vigezzi, *Phys. Rev. C* **72**, 011302(R) (2005).
 - [42] H. -C. Jean, J. Piekarewicz, and A. G. Williams, *Phys. Rev. C* **49**, 1981 (1994).
 - [43] T. Hatsuda, H. Shiomi, and H. Kuwabara, *Prog. Theor. Phys.* **95**, 1009 (1996).
 - [44] M. Matsuzaki and T. Tanigawa, *Phys. Lett.* **B445**, 254 (1999).
 - [45] P. Bożek, *Nucl. Phys.* **A657**, 187 (1999).
 - [46] M. Baldo and A. Grasso, *Phys. Lett.* **B485**, 115 (2000).
 - [47] U. Lombardo, P. Schuck, and W. Zuo, *Phys. Rev. C* **64**, 021301(R) (2001).